Molecular Therapy
Oncology
Original Article

Enhanced treatment of breast cancer brain metastases with oncolytic virus expressing anti-CD47 antibody and temozolomide

Jing Wang,[1,2,3,8] Lei Tian,[1,2,8] Tasha Barr,[1,2,8] Lewei Jin,[1,2,8] Yuqing Chen,[1,2] Zhiyao Li,[1,2] Ge Wang,[1,2] Jian-Chang Liu,[4] Li-Shu Wang,[1] Jianying Zhang,[5] David Hsu,[4] Mingye Feng,[6] Michael A. Caligiuri,[1,2,7] and Jianhua Yu[1,2,6,7]

[1]Department of Hematology & Hematopoietic Cell Transplantation, City of Hope National Medical Center, Los Angeles, CA 91010, USA; [2]Hematologic Malignancies Research Institute, City of Hope National Medical Center, Los Angeles, CA 91010, USA; [3]Department of Neurology, Xiangya Hospital, Central South University, Changsha, Hunan 410008, China; [4]Center for Biomedicine and Genetics, Beckman Research Institute of City of Hope, Los Angeles, CA 91010, USA; [5]Department of Computational and Quantitative Medicine, City of Hope National Medical Center, Los Angeles, CA 91010, USA; [6]Department of Immuno-Oncology, City of Hope, Los Angeles, CA 91010, USA; [7]City of Hope Comprehensive Cancer Center, Los Angeles, CA 91010, USA

Limited therapeutic options are available for patients with breast cancer brain metastases (BCBM), and thus there is an urgent need for novel treatment approaches. We previously engineered an effective oncolytic herpes simplex virus 1 (oHSV) expressing a full-length anti-CD47 monoclonal antibody (mAb) with a human IgG1 scaffold (OV-αCD47-G1) that was used to treat both ovarian cancer and glioblastoma. Here, we demonstrate that the combination of OV-αCD47-G1 and temozolomide (TMZ) improve outcomes in preclinical models of BCBM. The combination of TMZ with OV-αCD47-G1 synergistically increased macrophage phagocytosis against breast tumor cells and led to greater activation of NK cell cytotoxicity. In addition, the combination of OV-αCD47-G1 with TMZ significantly prolonged the survival of tumor-bearing mice when compared with TMZ or OV-αCD47-G1 alone. Combination treatment with the mouse counterpart of OV-αCD47-G1, termed OV-A4-IgG2b, also enhanced mouse macrophage phagocytosis, NK cell cytotoxicity, and survival in an immunocompetent model of mice bearing BCBM compared with TMZ or OV-A4-IgG2b alone. Collectively, these results suggest that OV-αCD47-G1 combined with TMZ should be explored in patients with BCBM.

INTRODUCTION

Breast cancer holds the title of being the most frequently diagnosed cancer on a global scale, and its prevalence has shown an upward trend in recent decades.[1] This disease is the leading cause of cancer mortality in women worldwide.[1] Breast cancer brain metastases (BCBM), the second most common solid tumor to involve the central nervous system, represent an important cause of morbidity and mortality among breast cancer patients, often leading to a poor prognosis.[2,3] With the improvement in developing systemic therapies, the incidence of brain metastases in metastatic breast cancer patients is reported to have decreased by 15%–35%.[4] Nevertheless, patients with BCBM have been at a disadvantage in large part by the lack of clinical research.[4] In fact, such patients are often excluded from clinical trials.[5] Presently, the established treatment protocols for individuals newly diagnosed with brain metastases may involve surgical intervention, stereotactic radiosurgery, whole brain radiotherapy, chemotherapy featuring agents capable of penetrating the central nervous system, or a blend of these approaches. However, achieving a cure still remains elusive.[4,5] Growing evidence from both preclinical and clinical data suggests that immunotherapeutic strategies, which leverage and amplify the activity of anti-tumor effector cells, are becoming more prominent,[6] such as immune checkpoint blockade and specific monoclonal antibody (mAb) therapy,[7–10] may provide additional benefit for patients with BCBM.

CD47, a transmembrane protein, acts as a "don't eat me" signal and is overexpressed in numerous types of tumor cells, including breast cancer.[6,11] CD47 establishes a signaling axis with its ligand, signal regulatory protein alpha (SIRPα), facilitating the evasion of tumor cells from macrophage-mediated phagocytosis.[12,13] Macrophages are certainly in abundance within a tumor as they can comprise up to half of a tumor mass,[14,15] and therefore anti-CD47 mAb therapy may provide a promising antitumor strategy for BCBM. Several clinical trials that include CD47-targeting agents are underway and have achieved impressive preliminary results in both liquid and solid malignancies.[16–18] Furthermore, the efficacy of an oncolytic herpes

Received 27 February 2024; accepted 31 May 2024;
https://doi.org/10.1016/j.omton.2024.200824.

[8]These authors contributed equally

Correspondence: Michael A. Caligiuri, Department of Hematology & Hematopoietic Cell Transplantation, City of Hope National Medical Center, Los Angeles, CA 91010, USA.
E-mail: mcaligiuri@coh.org
Correspondence: Jianhua Yu, Department of Hematology & Hematopoietic Cell Transplantation, City of Hope National Medical Center, Los Angeles, CA 91010, USA.
E-mail: jhyu1124@yahoo.com

simplex virus 1 (oHSV)-based strategy has been demonstrated in preclinical studies. Our approach involves engineering a transgene that expresses a full-length anti-CD47 mAb on a human IgG1 scaffold, previouly reported for the treatment of ovarian cancer and glioblastoma.[6,12] When delivered systemically, the full-length anti-CD47 mAb on a human IgG1 scaffold was proven to be relatively toxic, and a full-length anti-CD47 mAb on a human IgG4 scaffold was successfully developed to significantly reduce the inflammatory response presumably caused by the engagement of the IgG1 scaffold with the FcγR-bearing innate immune effector cells.[6,12] While both OV-αCD47-G1 and OV-αCD47-G4 hindered the macrophage "don't eat me" signal, only OV-αCD47-G1 significantly triggered both antibody-dependent cellular phagocytosis (ADCP) by macrophages and antibody-dependent cellular cytotoxicity (ADCC) by NK cells against these cancer cells.[6,12] Re-engineered oHSV is an excellent platform to deliver OV-αCD47-G1 locoregionally to solid tumors in the brain because the mAbs are produced beyond the blood-brain barrier following intratumoral administration of oHSV, thus avoiding the systemic toxicity, yet allowing for both ADCP and ADCC within the central nervous system.[6,19,20] The three distinct modes of cell killing used by the re-engineered oHSV combined with chemotherapy represents a promising and practical strategy to improve therapeutic efficacy.[21,22]

Temozolomide (TMZ), a cytotoxic DNA alkylating agent with mutagenic potential, is the most commonly used chemotherapeutic agent for treating glioblastoma.[23] TMZ is the current standard of care for glioblastoma; however, there is potential immune modulation by TMZ, such as induction of lymphopenia, increased proportion of regulatory T cells, and enhanced dendritic cell function and proliferation of antigen-specific T cells.[24] Thus, TMZ is reported to either synergize or antagonize with oHSV.[21,25,26] Given the immune stimulating effects of our constructs,[6,19,20] we hypothesized that combination of systemically administered TMZ and our oHSV construct would exhibit therapeutic synergy, especially as the latter has a payload to overcome immune suppression rendered by checkpoints such as the SIRPα-CD47 axis.

In this study, we paired TMZ with an oncolytic virus (OV) carrying a full-length, soluble anti-CD47 antibody utilizing a human IgG1 scaffold (OV-αCD47-G1) or IgG4 scaffold (OV-αCD47-G4) to assess our hypothesis. When compared with OV-αCD47-G1 alone, TMZ combined with OV-αCD47-G1 also activated human NK cell cytotoxicity and macrophage phagocytosis. Finally, in mouse models intracranially engrafted with human or mouse breast tumor cells, the administration of TMZ with either OV-αCD47-G1 or its mouse counterpart, OV-A4-IgG2b, significantly inhibited local tumor growth and prolonged overall survival.

RESULTS

Both OV-αCD47-G1- and OV-αCD47-G4-infected MDA-MB-231 cells secrete a full-length anti-CD47 antibody

We utilized αCD47-G1, αCD47-G4, and oHSV expressing either of the full-length antibodies, as reported previously.[6,13] Both αCD47-G1 and αCD47-G4 in the oHSVs are driven by the immediately early gene promoter IE4/5 of the virus to achieve a high-level expression after infection.[6,13] The results of a CD47 blocking assay demonstrated similar dose-dependent CD47 blocking capacity for both αCD47-G1 and αCD47-G4 (Figure 1A). The anti-CD47 antibody yield from OV-αCD47-G1- and OV-αCD47-G4-infected human breast cancer MDA-MB-231 cells was quantified by enzyme-linked immunosorbent assay (ELISA) and demonstrated considerable and comparable quantities of secreted anti-CD47 antibody were observed as early as 12 h post-infection (hpi), reaching nearly maximal levels exceeding 5 μg/mL at 24 hpi, with peak levels achieved (Figure 1B).

We then investigated the cytotoxic effects of TMZ either alone or in combination with OV-Q1, OV-αCD47-G1, or OV-αCD47-G4 treatment *in vitro*. First, a dose titration was performed with TMZ and MDA-MB-231 cells. We measured cell death over 72 h and found that MDA-MB-231 cells were sensitive to the TMZ treatment (Figure 1C). We next assessed the viability of MDA-MB-231 cells following exposure to either OV-Q1, OV-αCD47-G1, or OV-αCD47-G4 at varying multiplicity of infection (MOI). We did not observe any differences in viability among viruses (Figure 1D). To evaluate the effect of treatment with both oHSVs and TMZ, MDA-MB-231 cells were pre-treated with 40 μM TMZ for 6 h as reported previously.[27] Next, cells were either exposed to OV-Q1, OV-αCD47-G1, or OV-αCD47-G4 at an MOI of 0.1 or treated with both TMZ and each respective virus for 12 h. The combination of an oHSV and TMZ resulted in superior lysis of MDA-MB-231 cells compared with single treatments (Figure 1E). Finally, we evaluated the impact of TMZ treatment on the viral production of OV-Q1, OV-αCD47-G1, and OV-αCD47-G4. To do so, we treated cells with their respective combinations alongside TMZ for 48 h. The viral production of treated cells was measured by a plaque assay with Vero cells. Our data showed that TMZ had no effect on viral production (Figure 1F).

TMZ augments phagocytosis induced by αCD47-G1 released from breast cancer cells infected with OV-αCD47-G1, which impeds "don't eat me" signaling in macrophages

We next compared the capacity of αCD47-G1 and αCD47-G4 to modulate the phagocytosis of human MDA-MB-231 cells by both mouse and human macrophages, in the presence or absence of TMZ. We used mouse bone marrow-derived macrophages (BMDMs) isolated from BALB/c mice as effector cells.[6,12] Flow cytometric analysis showed that TMZ alone enhanced the BMDM phagocytosis against MDA-MB-231 cells (Figures S1A and S1B). Moreover, when combined with TMZ, both αCD47-G1 and αCD47-G4 purified from transduced CHO cells resulted in significantly higher levels of BMDM phagocytosis against MDA-MB-231 cells compared with their respective individual treatments (Figures S1A and S1B).

The phagocytosis assessement with BMDMs was also repeated with unconcentrated supernatants obtained from OV-αCD47-G1-, OV-αCD47-G4-, or OV-Q1-infected MDA-MB-231 cells. αCD47-G1 in the supernatant from infected cells exhibited over a 2-fold increase

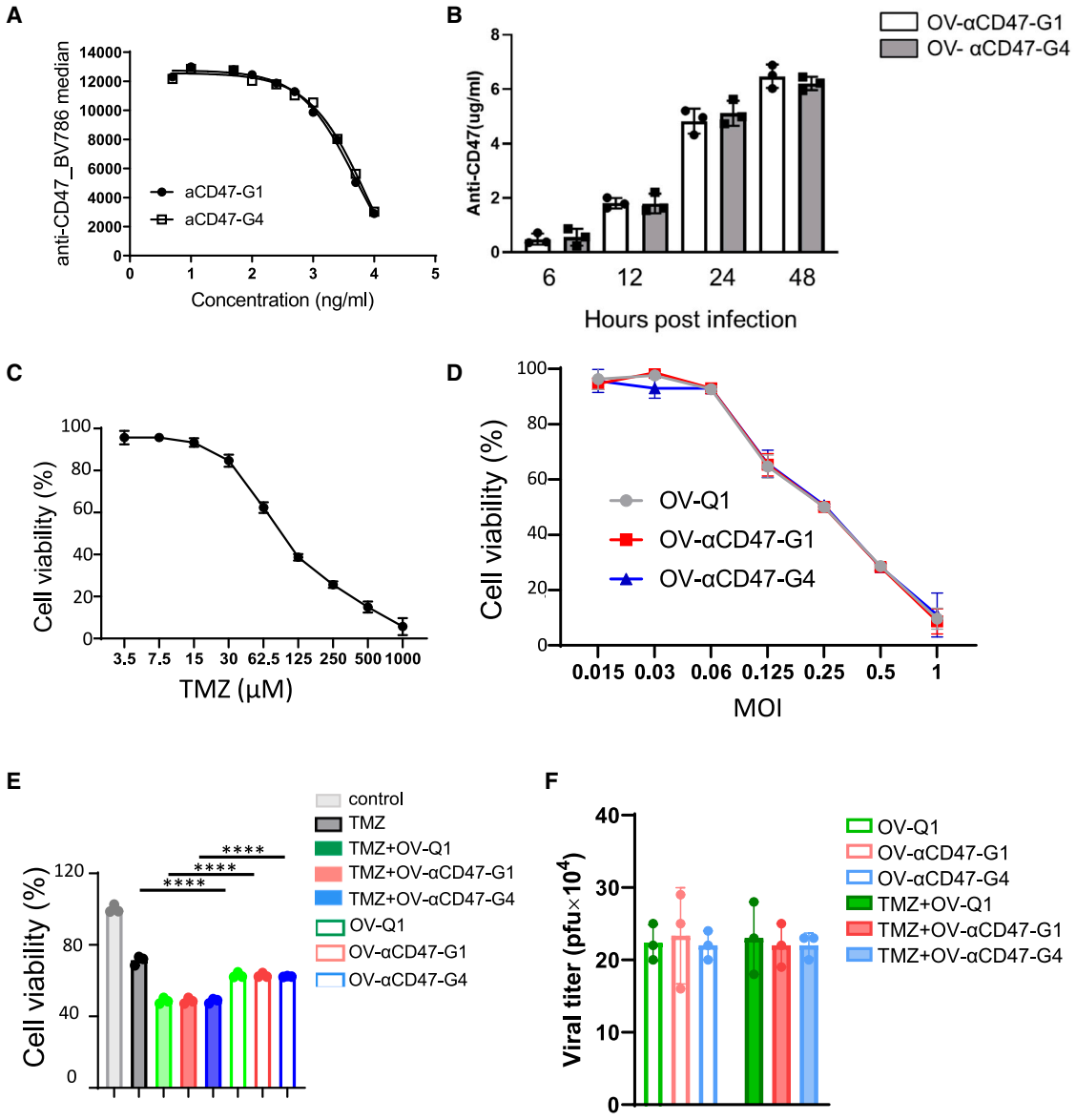

Figure 1. Characterization of OV-Q1, OV-αCD47-G1, and OV-αCD47-G4 and their combinational effect with TMZ

(A) Blocking of anti-CD47 monoclonal antibody (mAb) binding by αCD47-G1 and αCD47-G4 mAbs. MDA-MB-231 cells were exposed to increasing concentrations of αCD47-G1 or αCD47-G4 mAbs obtained from CHO cell culture. Subsequently, the cells were treated with a conjugated anti-human CD47 antibody and analyzed using flow cytometry. (B) Determination of αCD47-G1 and αCD47-G4 yields from supernatants of OV-αCD47-G1- and OV-αCD47-G4-infected MDA-MB-231 cells through ELISA assay. (C) Assessment of TMZ cytotoxicity against MDA-MB-231 cells at specified doses using the CellTiter-Glo 2.0 assay. (D) Analysis of cell lysis in MDA-MB-231 cells infected with OV-Q1, OV-αCD47-G1, or OV-αCD47-G4 at the indicated multiplicity of infection (MOI) levels at 48 h post infection, measured by the CellTiter-Glo 2.0 assay. (E) Evaluation of cell lysis in MDA-MB-231 cells, treated with or without TMZ, and subsequently infected with OV-Q1, OV-αCD47-G1, or OV-αCD47-G4. Cell lysis was assessed using the CellTiter-Glo 2.0 assay. (F) Viral replication in MDA-MB-231 cells treated with or without TMZ and infected with OV-Q1, OV-αCD47-G1, or OV-αCD47-G4 at an MOI of 2. The supernatants were collected 48 h post-infection for viral reproduction analysis using a plaque assay in Vero cells. Error bars indicate the standard deviations (SD). All data are presented as mean ± SD. ****$p \leq 0.0001$.

in macrophage phagocytosis against breast cancer cells compared with the αCD47-G4 supernatant, consistent with the earlier observation. Finally, the combination of supernatant from OV-αCD47-G1 infection and TMZ yielded the highest levels of macrophage phagocytosis compared with either single treatment alone or compared with TMZ plus supernatants from either OV-Q1 or OV-αCD47-G4 infection (Figures S1C and S1D).

We next evaluated the effect of treatments on cytokine expression in macrophages. We found that, in mouse BMDMs, αCD47-G1

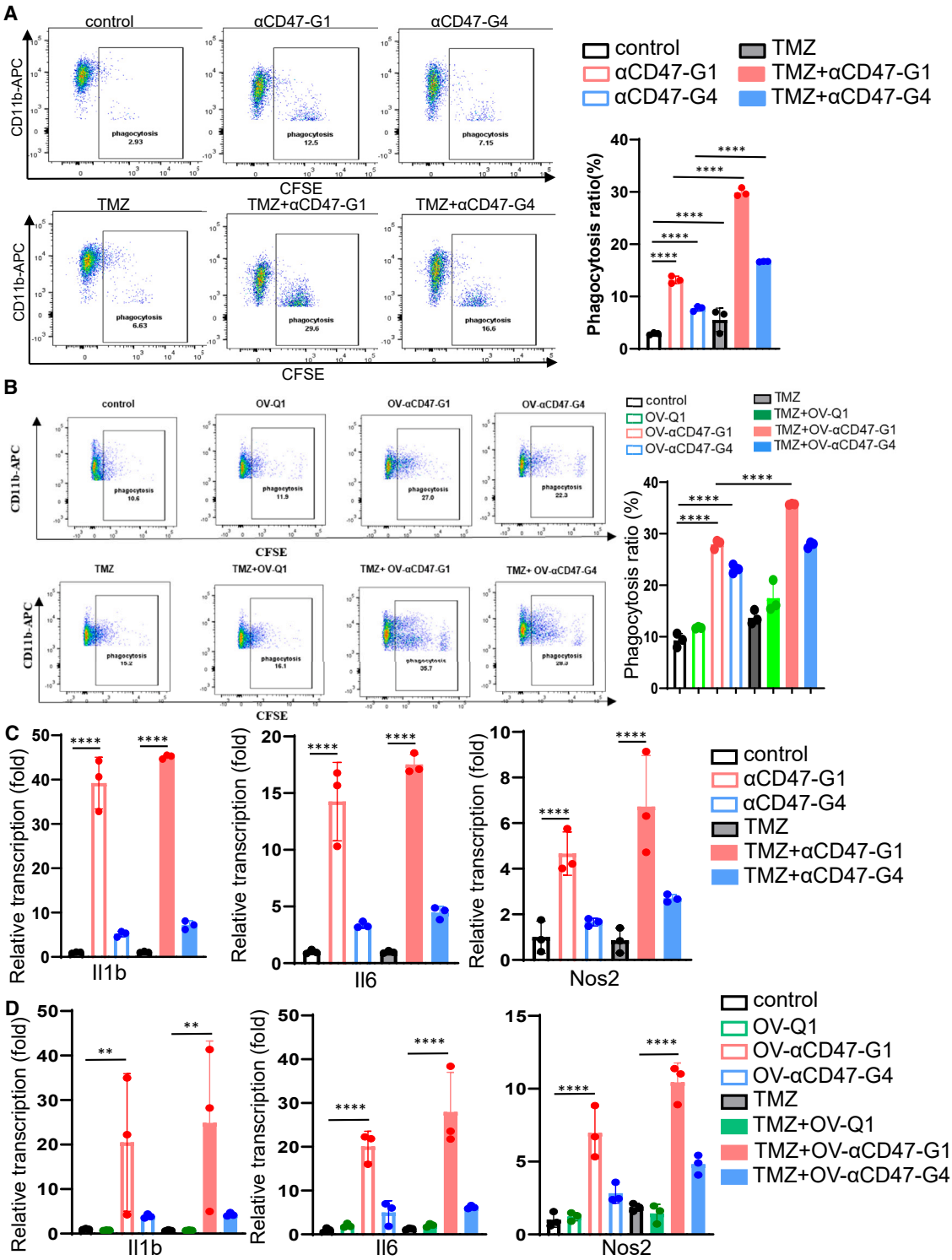

Figure 2. αCD47-G1 plus TMZ enhances human macrophage ADCP against breast cancer cells

(A) MDA-MB-231 cells, pre-treated with or without TMZ, were labeled with CFSE and co-cultured with human macrophages at an effector to target ratio of 1:2. This co-culture was conducted in the presence of a vehicle control, αCD47-G1, or αCD47-G4 produced by CHO cells, each at a dose of 5 μg/mL. The flow cytometry assay was utilized to determine the percentage of human macrophage phagocytosis against MDA-MB-231 cells ($CD11b^{+}CFSE^{+}$). (B) MDA-MB-231 cells, pre-treated with or without

(legend continued on next page)

(produced by CHO cells and then purified) when combined with TMZ dramatically induced the transcription of both typical macrophage inflammatory cytokine and chemokine genes such as *Il1b*, *Il6*, *Il12*, *Ccl2*, *Ccl4*, and *Nos2* (Figure S2A). These genes were previously reported to be upregulated in response to IgG1 antibody.[28] We observed similar results for αCD47-G1 supernatants from OV-αCD47-G1-infected MDA-MB-231 cells combined with TMZ (Figure S2B). However, the combination of αCD47-G4 and TMZ had no such effect (Figure S2A).

The impact of combining αCD47-G1 with TMZ on the stimulation of human macrophage phagocytosis was also evaluated. In this regard, primary human donor-derived macrophages were employed as effector cells, as documented previously.[29] In comparison with vehicle control, similar to mouse BMDMs, αCD47-G1, purified from transduced CHO cells, combined with TMZ significantly enhanced the phagocytosis of human macrophages against MDA-MB-231 cells (Figure 2A). Comparable outcomes were observed with unpurified supernatants obtained from OV-αCD47-G1- or OV-αCD47-G4-infected MDA-MB-231 cells. Both αCD47-G1, released by OV-αCD47-G1-infected cells, and αCD47-G4, released by OV-αCD47-G4-infected cells, markedly increased the phagocytosis of MDA-MB-231 cells by human macrophages when combined with TMZ, in comparison with their respective standalone effects (Figure 2B). Among all the tested conditions, the combination of αCD47-G1, secreted by OV-αCD47-G1-infected cells, with TMZ demonstrated the most pronounced effect. In addition, treatment of human macrophages with αCD47-G1 also activated the transcription of typical macrophage cytokine genes such as *Il1b*, *Il6*, and *Nos2* (Figure 2C); however, the addition of TMZ to αCD47-G1 resulted in a more significant transcriptional change. Similar results were obtained when using αCD47-G1 secreted by OV-αCD47-G1-infected MDA-MB-231 cells. The addition of TMZ led to the most pronounced activation of both cytokine and chemokine genes (Figure 2D).

αCD47-G1 released by OV-αCD47-G1-infected breast cancer cells combined with TMZ triggers robust NK cell-mediated ADCC

NK cells exert an antitumor function due to their inherent cytotoxicity and ability to induce ADCC in the presence of specific antibodies. As we reported previously, OV-αCD47-G1 stimulates the anti-tumor response of human NK cells through ADCC against glioblastoma and metastatic ovarian cancer.[6,12] To assess the impact of αCD47-G1 and TMZ on the antitumor activity of human NK cells, we conducted cytotoxicity assays employing freshly isolated human NK cells as effector cells and MDA-MB-231 breast cancer cells as target cells, which were either pre-treated with or without TMZ. The results showed that the combination of αCD47-G1 with TMZ, but not αCD47-G1 alone or αCD47-G4 combined with TMZ, effectively triggered robust NK cell-mediated ADCC against breast cancer cells (Figure 3A). There was only baseline cytotoxicity with αCD47-G4 combined with TMZ presumably. This is because αCD47-G4 does not engage the FcγRIII expression as CD16 on NK cells. This experiment was repeated with supernatants from OV-Q1-, OV-αCD47-G1-, and OV-αCD47-G4-infected MDA-MB-231 cells. Consistent with the findings of macrophage phagocytosis, supernatant from OV-αCD47-G1-infected MDA-MB-231 breast cancer cells induced the strongest NK cell-induced cytotoxicity targeting MDA-MB-231 cells pre-treated with TMZ (Figure 3B).

Furthermore, in the presence of tumor cells, the combination of purified αCD47-G1 secreted by CHO cells and TMZ markedly enhanced the surface expression of the activation markers CD69 and CD107a on NK cells, in comparison with the individual agents. However, such an effect was not observed in the combination of purified αCD47-G4, secreted by CHO cells, and TMZ (Figure S3). Purified αCD47-G1, secreted by CHO cells, combined with TMZ also significantly increased the production of granzyme B, TNF-α, and IFN-γ beyond that seen by either factor alone (Figure S3). Similar results were observed when using supernatants released from OV-Q1-, OV-αCD47-G1-, and OV-αCD47-G4-infected MDA-MB-231 cells to treat MDA-MB-231 cells that were pre-treated with or without TMZ (Figure 3C). In addition, TMZ plus OV-αCD47-G1 resulted in the most significant changes compared with other single and combination therapies (Figure 3C).

OV-αCD47-G1 combined with TMZ improves oncolytic virotherapy and prolongs survival in a xenograft BCBM model

To evaluate the efficacy of OV-αCD47-G1 combined with TMZ against BCBM *in vivo*, we utilized an orthotopic model of human BCBM by intracranially injecting (i.c.) 1×10^5 MDA-MB-231 cells into athymic nude mice on day 1.[30] One week following tumor implantation, the animals were administered i.c. with OV-αCD47-G1, OV-αCD47-G4, or OV-Q1 at a dosage of 2×10^5 PFU per mouse, while the control group received a saline placebo. TMZ (100 mg/kg) was intraperitoneally injected daily from days 7 to 14, and tumor progression was monitored. OV-αCD47-G1 and OV-αCD47-G4 notably extended median survival (Figure 4). While TMZ alone did not significantly prolong median survival, the combination of OV-αCD47-G1 with TMZ demonstrated superior efficacy compared

TMZ, were labeled with CFSE and co-cultured with human macrophages at an effector to target ratio of 1:2. The co-culture was carried out in the presence of a vehicle control, conditioned media from OV-Q1-, OV-αCD47-G1-, and OV-αCD47-G4-infected MDA-MB-231 cells. The flow cytometry assay was employed to assess the percentage of primary human macrophage phagocytosis against MDA-MB-231 cells ($CD11b^+CFSE^+$). (C) Primary human macrophages were co-cultured with MDA-MB-231 cells, pre-treated with or without TMZ, at a ratio of 1:1. This co-culture was performed in the presence or absence of αCD47-G1 or αCD47-G4 produced by CHO cells for 6 h, followed by gene transcript quantification using RT-qPCR. (D) Primary human macrophages were co-cultured with MDA-MB-231 cells, pre-treated with or without TMZ, at a ratio of 1:1. The co-culture was conducted in the presence of control medium or conditioned medium from the culture of OV-Q1-, OV-αCD47-G1-, or OV-αCD47-G4-infected MDA-MB-231 cells for 6 h, followed by gene transcript quantification using RT-qPCR. All experiments were performed with three donors. Error bars represent standard deviations of means of three donors. One-way ANOVA with p values was corrected for multiple comparisons by the Bonferroni test. $^{**}p \leq 0.01$, $^{****}p \leq 0.0001$.

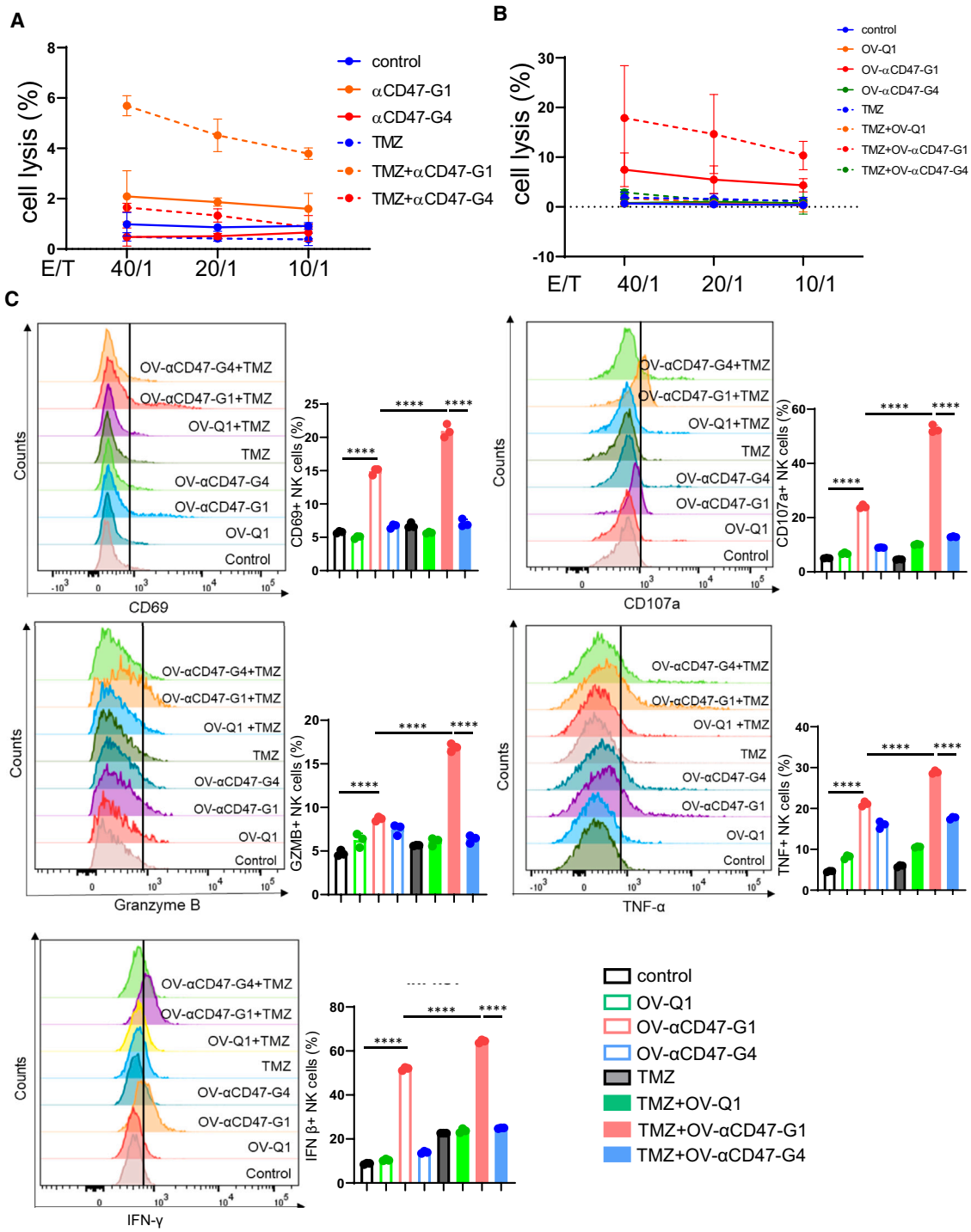

Figure 3. αCD47-G1 plus TMZ increases human NK cell-mediated ADCC against breast cancer cells

(A) Assessment of cytotoxicity exhibited by human primary NK cells against MDA-MB-231 cells treated with αCD47-G1 and αCD47-G4, with or without prior TMZ pre-treatment. (B) Evaluation of cytotoxicity displayed by human primary NK cells against MDA-MB-231 cells, pre-treated with or without TMZ, in the presence of either control medium or conditioned medium from the culture of OV-Q1-, OV-αCD47-G1-, or OV-αCD47-G4-infected MDA-MB-231 cells. (C) Investigation into the impact of αCD47-G1 or αCD47-G4 on the expression of NK cell activation markers (CD69, CD107a, granzyme B, TNF-α, and IFN-γ) during co-culture with MDA-MB-231 cells pre-treated with or without TMZ, maintaining an effector to target ratio of 1:1. All experiments were conducted with three donors, and error bars indicate standard deviations of means from the three donors. One-way ANOVA with p values was corrected for multiple comparisons by the Bonferroni test. ****$p \leq 0.0001$.

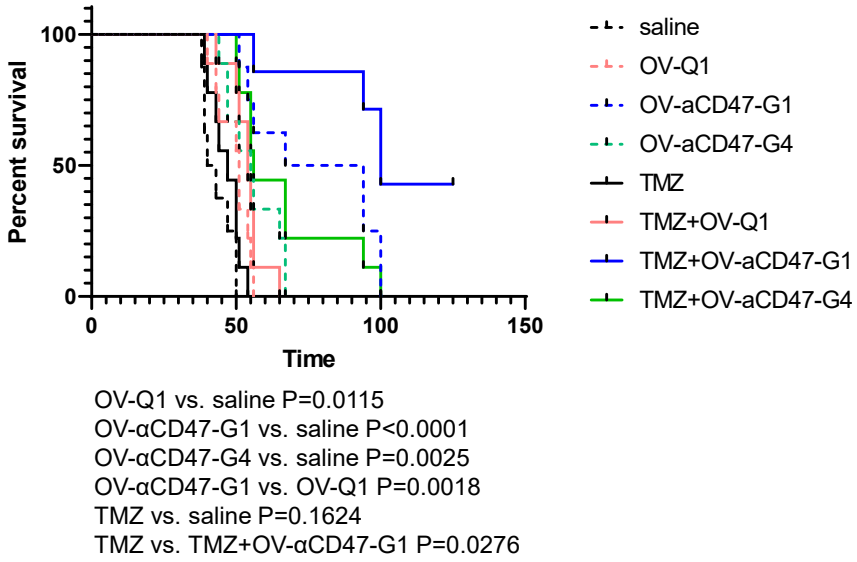

Figure 4. OV-αCD47-G1 combined with TMZ improves oncolytic virotherapy in a xenograft BCBM animal model

Survival analysis of mice bearing MDA-MB-231 tumors, subjected to treatment with OV-Q1, OV-αCD47-G1, or OV-αCD47-G4, with or without TMZ. Kaplan-Meier methodology was employed for survival estimation, and the results were compared using the log rank test (n = 6 independent mice).

with other single treatments and combination therapies in achieving this effect (Figure 4).

OV-A4-IgG2b combined with TMZ is superior to single treatments in improving outcome in a fully immunocompetent BCBM model

We established a fully immunocompetent mouse model by substituting the anti-human CD47 antibody with the anti-mouse CD47 antibody as reported previously.[6,13] In brief, we utilized anti-mouse CD47 antibodies (clone A4)[31] on mouse IgG2b (equivalent to human IgG1 for Fc receptor binding) and mouse IgG3 (similar to human IgG4 for Fc receptor binding) scaffolds, termed A4-IgG2b and A4-IgG3, respectively. The corresponding oHSV constructs were named OV-A4-IgG2b and OV-A4-IgG3. We found that A4-IgG2b, purified from transduced CHO cells, induced significantly higher levels of BMDM phagocytosis against E0771 mouse breast cancer cells that were pre-treated with TMZ, in comparison with the effects observed with either reagent alone (Figure 5A). Similar results were observed when co-culturing macrophages with E0771 cells pre-treated either with or without TMZ in the unconcentrated supernatants from OV-A4-IgG2b-, OV-A4-IgG3-, or OV-Q1-infected E0771 cells (Figure 5B).

To determine the effect of A4-G2b, the mouse equivalent of αCD47-G1, in combination with TMZ on mouse NK cell antitumor activity, we employed mouse NK cells isolated from C57BL/6 mice as effector cells, while E0771 mouse breast cancer cells treated with or without TMZ were used as target cells. We found that the combination of A4-G2b, secreted from CHO cells, with TMZ also enhanced the cytotoxicity of mouse NK cells in comparison with individual agents alone (Figure 5C). Similar results were obtained when co-culturing macrophages with E0771 cells pre-treated either with or without TMZ in the unconcentrated supernatants from OV-A4-IgG2b-infected E0771 cells (Figure 5D).

To evaluate the antitumor effect of TMZ combined with OV-A4-G2b treatment *in vivo*, we used C57BL/6 mice i.c. injected with E0771 cells in a survival study. Four days after implantation with 1×10^5 E0771 cells, mice were intratumorally injected with either OV-Q1, OV-A4-IgG2b, OV-A4-IgG3, or vehicle control. From days 4 to 11, mice received once daily intraperitoneal injections of TMZ (100 mg/kg). The findings indicate a substantial increase in the median survival of mice treated with OV-A4-IgG2b, OV-A4-IgG3, and TMZ alone. However, the combination of OV-A4-G2b with TMZ led to the most significant extension in median survival compared with the other groups (Figure 6A).

To elucidate the immunological mechanisms contributing to the therapeutic impact of OV-A4-IgG2b when combined with TMZ, we conducted a flow cytometry assay to investigate immune cell recruitment and activation. The findings indicated that, in comparison with individual treatments or other combination groups, the combination of OV-A4-IgG2b with TMZ resulted in the highest recruitment of macrophages and NK cells (Figures 6B and 6C). Likewise, combining OV-A4-IgG2b and TMZ resulted in the greatest NK cell activation with a higher CD69 expression, and enhanced macrophage antitumoral polarization by decreasing CD206 expression (Figures 6D and 6E).

DISCUSSION

CD47 exhibits elevated expression on the surface of various tumor cells, including those associated with breast cancer.[11] We have shown that CD47 binds to its receptor SIRPα on the surface of macrophages in *in vivo* models of glioblastoma and metastatic ovarian cancer.[6,12] This interaction leads to a "don't eat me" signal to macrophages, aiding in shielding the tumor cells from elimination. Consistent with this concept, we demonstrated that the use of anti-CD47 antibodies with TMZ enhances the phagocytosis of cancer cells, which is consistent with work by Gholamin et al.[32] who also found that combining CD47 blockade with TMZ results in a significant pro-phagocytosis effect. TMZ is a cytotoxic DNA alkylating agent with mutagenic potential and one of only a few systemically delivered chemotherapy options proven to improve survival in patients with glioblastoma.[33–35] Unfortunately, previous studies[36,37] have shown disappointing activity for TMZ as a single-agent therapy in BCBM.[38]

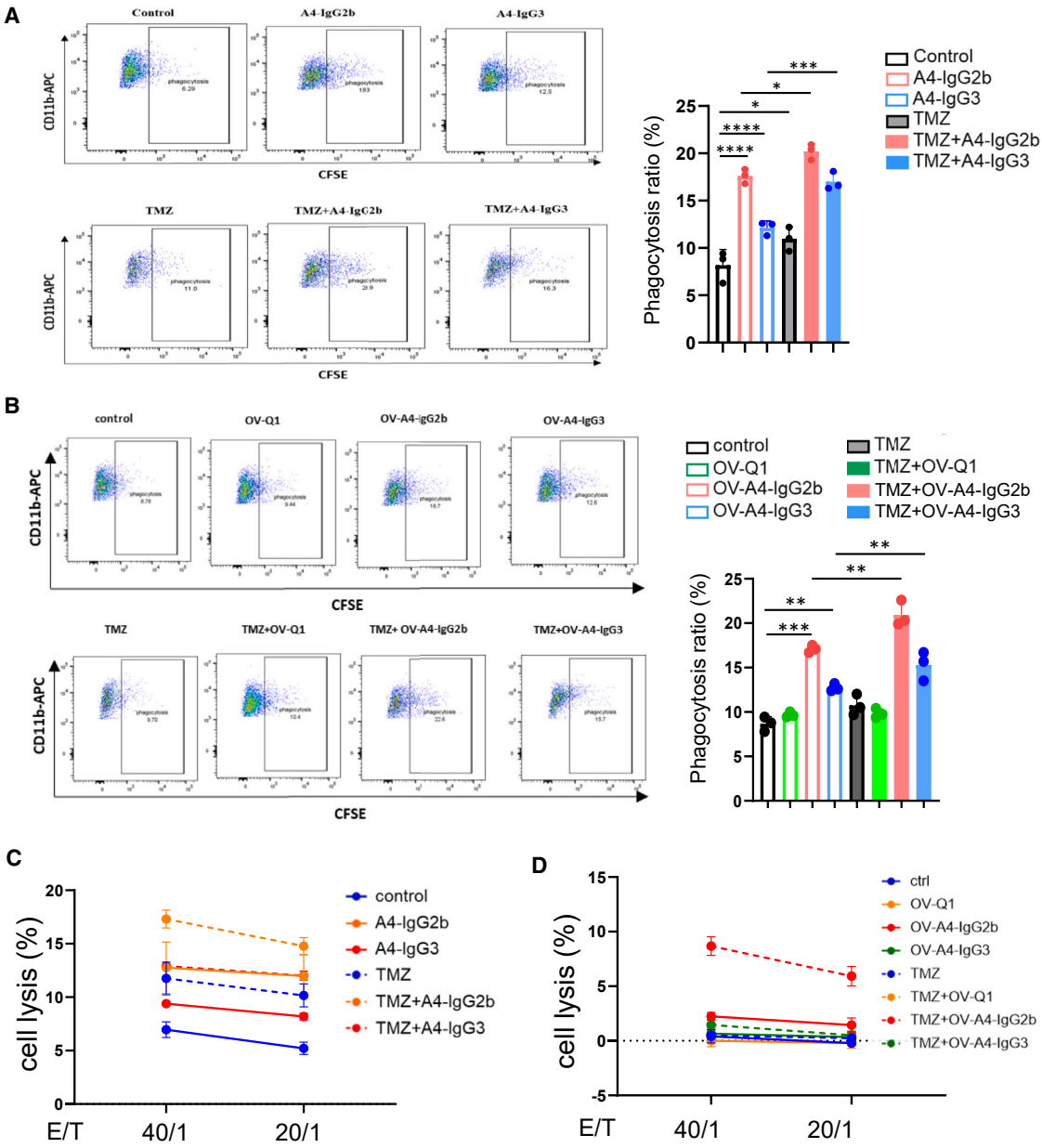

Figure 5. A4-IgG2b plus TMZ promotes mouse macrophage and NK cell activation

(A) E0771 cells, treated with or without TMZ, were labeled with CFSE and co-cultured with mouse BMDMs at an effector to target ratio of 1:2. This co-culture was conducted in the presence of a vehicle control, A4-IgG2b, or A4-IgG3 produced by CHO cells, each at a dose of 5 μg/mL. The flow cytometry assay was employed to determine the percentage of BMDM phagocytosis against E0771 cells ($CD11b^+CFSE^+$). (B) E0771 cells, pre-treated with or without TMZ, were labeled with CFSE and co-cultured with mouse BMDMs at an effector to target ratio of 1:2. The co-culture was carried out in the presence of a vehicle control, or conditioned media from OV-Q1-, OV-A4-IgG2b-, or OV-A4-IgG3-infected E0771 cells. The flow cytometry assay was utilized to assess the percentage of BMDM phagocytosis against E0771 cells ($CD11b^+CFSE^+$). (C) Evaluation of cytotoxicity displayed by mouse primary NK cells against E0771 cells treated with A4-IgG2b and A4-IgG3, with or without prior TMZ pretreatment. (D) Assessment of cytotoxicity exhibited by mouse primary NK cells against E0771 cells, pre-treated with or without TMZ, in the presence of either control medium or conditioned media from the culture of OV-Q1-, OV-A4-IgG2b-, or OV-A4-IgG3-infected E0771 cells. All experiments were conducted with three donors, and error bars indicate standard deviations of means from the three donors. One-way ANOVA with p values was corrected for multiple comparisons by the Bonferroni test. $^*p \leq 0.05$, $^{**}p \leq 0.01$, $^{***}p \leq 0.001$, $^{****}p \leq 0.0001$.

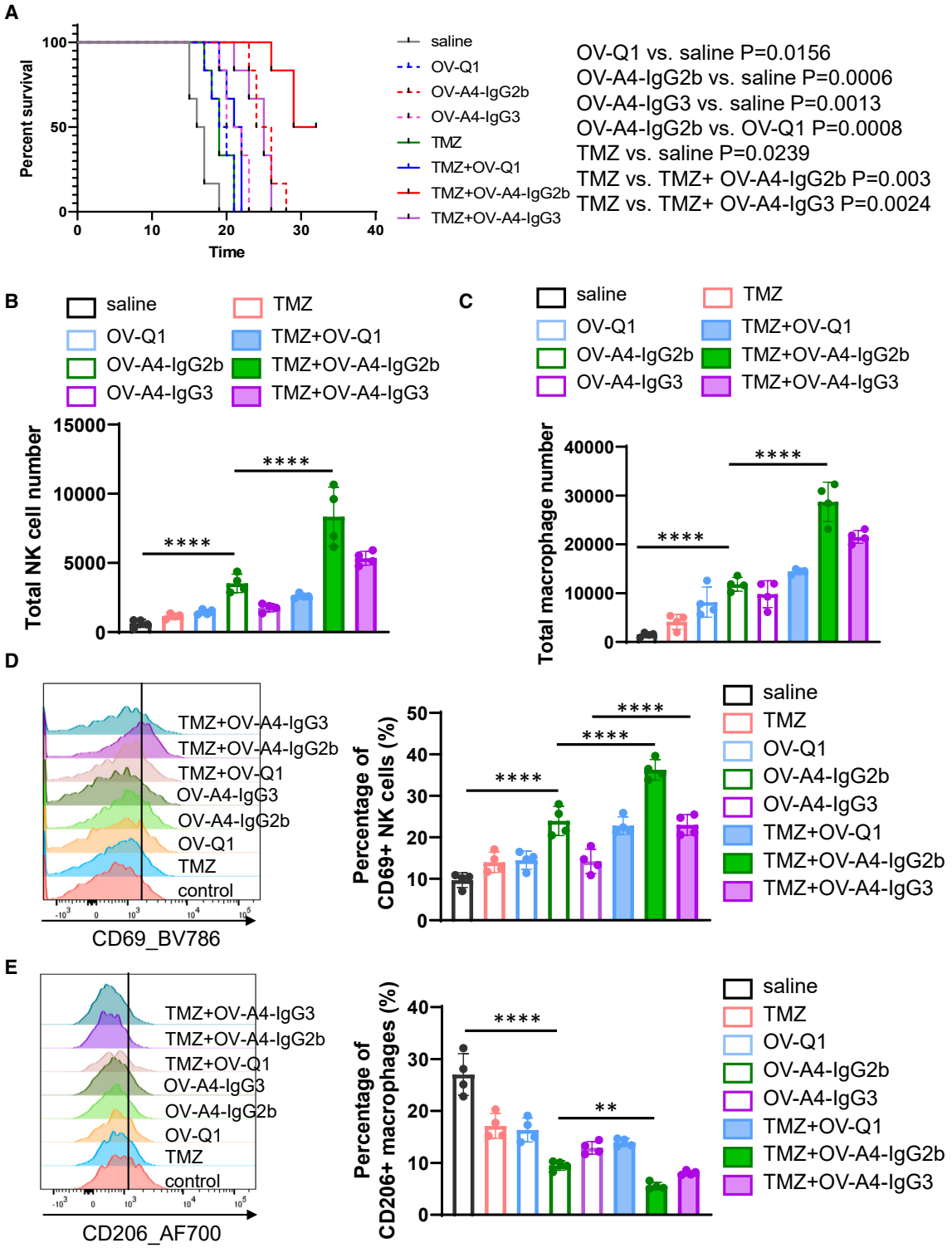

Figure 6. OV-A4-IgG2b plus TMZ is superior to the single treatments in improving outcomes in a fully immunocompetent BCBM model

(A) Assessment of the survival of C57BL/6 immunocompetent mice bearing E0771 tumors following treatment with vehicle control, OV-Q1, OV-A4-IgG2b, or OV-A4-IgG3, either alone or in combination with TMZ. (B and C) Flow cytometry analysis of intracranial infiltration of NK cells ($CD3^{-}NKp46^{+}$) (B) and macrophages

(legend continued on next page)

Herpes simplex type I is a neurotropic DNA virus, which, left unchecked, can result in a lethal encephalitis.[39] We have previously reported on the use of a modified oncolytic herpes simplex virus (oHSV) termed rQNestin34.5 and, using this as a backbone, created a number of constructs each of which secreted various forms of Ig, described within the methods. In this study, we used a novel combination to treat experimental BCBM: an OV expressing a full-length αCD47 mAb that is secreted to provide an innovative antibody delivery system designed to augment anti-tumor responses when delivered in combination with TMZ. We created both OV-αCD47-G1 and OV-αCD47-G4 constructs, which were designed to regionally secrete an αCD47-G1 and αCD47-G4 antibody, respectively, directly into the breast cancer brain metastasis tumor microenvironment after a single intratumoral injection of the virus. We integrated these constructs with the FDA-approved chemotherapeutic agent TMZ to create a novel treatment approach for breast cancer patients with brain metastases. When OV-αCD47-G1 was paired with TMZ, the αCD47 antibody regionally generated by OV-infected cells effectively inhibited the heightened "don't eat me" signal facilitated by the interplay between SIRPα on macrophages and CD47 on breast tumor cells. Furthermore, we found that our engineered OV-αCD47-G1 not only directly lysed tumor cells but also activated NK cell ADCC and macrophage ADCP function in *in vitro* models for glioblastoma and metastatic ovarian cancer.[6,12] Moreover, TMZ enhanced OV-αCD47-G1's ability to further activate NK cell ADCC. Hence, the combination of TMZ with OV-αCD47-G1 markedly enhanced the effectiveness of virotherapy against breast tumors *in vivo*.

Previous research has investigated the combination of αCD47 and TMZ in cancer treatment. For instance, a study highlighted that TMZ countered oncolytic immunovirotherapy (G47Δ-mIL12, a herpes oncolytic virus with the deletion of the ICP47 viral gene while expressing mouse IL-12) in glioblastoma.[21] In addition, another research showcased the synergistic inhibition of breast cancer cell tumorigenesis through the combination of oncolytic herpes simplex virus (G47Δ) and TMZ.[26] Furthermore, a separate study emphasized the synergistic effect of oncolytic virus (G47Δ) and TMZ in targeting glioblastoma stem cells by manipulating DNA damage responses.[25] However, the specific approach of blocking CD47 using an antibody produced by an OV-infected tumor cell, along with using IgG1 from an αCD47 antibody to regulate FcR-mediated effects in both macrophages and NK cells, has never been discussed previously in the setting of BCBMs. In our study, we not only investigated the phagocytic activity of macrophages but also delved into the functional role of NK cells. It is worth noting that a recent study demonstrated the upregulation of SIRPα in NK cells upon IL-2 stimulation, highlighting the existence of a SIRPα-CD47 immune checkpoint that exits in NK cells.[40] Thus, like macrophages, IgG1 αCD47 antibodies in the setting of NK cells can play a role in both triggering Fc receptors and blocking the "don't eat me" signal.

Macrophages play key roles in tumor progression and can even comprise half the tumor mass within the brain or breast.[14,15,41] By secreting various cytokines or growth factors, they are capable of inducing angiogenesis, promoting tumor cell invasion, and even enhancing immune cell infiltration into the tumor microenvironment. We found that TMZ combined with OV-αCD47-G1 not only improves phagocytosis but can also increase the expression of several cytokines, chemokines, or growth factors such as *IL-1β*, *IL6*, *IL12*, *CCL2*, *CCL4*, and *NOS2*. It has been reported that TMZ can induce tumor cell ER stress.[42] The tumor cells with increased ER stress might activate macrophages compared with normal tumor cells.[43] However, it is possible that unidentified additional multiple mechanisms might also contribute to the heightened therapeutic impact resulting from the combination of anti-CD47 with TMZ. For instance, increasing pro-phagocytic signals might improve anti-CD47 effects. Chao et al. demonstrated pro-phagocytic "eat me" signals (such as calreticulin) can enhance macrophage-mediated tumor phagocytosis mediating by anti-CD47 antibodies and potentially enhance patient outcomes.[36]

ADCC is widely recognized as a major mechanism of action for many anti-cancer antibody therapies, with NK cells playing a significant role in mediating cytotoxicity.[44] Supporting this notion, clinical data have shown a positive correlation between intratumoral NK cell presence and patient outcomes including survival.[37,45] ADCC relies on the interactions between the antibody Fc domains and Fc receptors expressed by specific leukocyte populations. Our results demonstrated that OV-αCD47-G1 and OV-A4-IgG2b, are more effective in prolonging the survival of mice carrying BCBM tumors compared with OV-αCD47-G4 and OV-A4-G3. Some studies have shown that combination therapies with TMZ improve ADCC, which allows for lower doses of TMZ to be used without compromising therapeutic efficacy.[44,46] In the current study, we found that breast cancer cells pre-treated with TMZ improved the ADCC mediated by OV-αCD47-G1 and OV-A4-IgG2b.

In summary, we have utilized a novel and effective oHSV-based approach to treat BCBM via engineering a transgene expressing a full-length anti-CD47 mAb on an IgG1 scaffold in combination with TMZ. This is a unique approach for improving control of breast cancer brain metastasis treatment via enhancing anti-tumor innate immunity.

METHODS

Ethics statement

Experiments and handling of mice were conducted under federal, state, and local guidelines and with an approval from the City of Hope Institutional Animal Care and Use Committee. Peripheral blood cones were collected from healthy donors to isolate human monocytes and NK cells, after written informed consent in the City

(F4/80^{+}CD45^{high}CD11b^{+}) (C) in E0771-bearing mice 3 days after virus injection (n = 4 animals). (D and E) Quantification of CD69 expression in NK cells (D) and CD206 expression in macrophages (E) subsequent to combination therapy. For (B)–(E), one-way ANOVA with p values corrected for multiple comparisons by the Bonferroni test. Data are presented as mean values ± SD. $^{**}p \leq 0.01$, $^{****}p \leq 0.0001$.

of Hope Michael Amini Transfusion Medicine Center under institutional review board-approved protocols.

Cells

Vero cells were obtained from the laboratory of E. Antonio Chiocca. MDA-MB-231, E0771, and CHO cells were originally purchased from ATCC. MDA-MB-231 human breast cancer cell lines and E0771 mouse breast cancer cells were cultured with DMEM supplemented with 10% FBS, penicillin (100 U/mL), and streptomycin (100 μg/mL). Monkey kidney epithelium-derived Vero cells used for viral propagation and plaque-assay-based viral titration were maintained with DMEM supplemented with 10% FBS, penicillin (100 U/mL), and streptomycin (100 μg/mL). No further authentication of these cell lines was performed. Cell morphology and growth characteristics were monitored during the study and compared with published reports to ensure their authenticity. All cell lines used in this study were determined to be negative for mycoplasma prior to experiments using the MycoAlert Mycoplasma Detection Kit (Lonza, cat. no. LT07-318). All cell lines were used within 10 passages after thawing.

Production of αCD47-G1, αCD47-G4, A4-IgG2b, and A4-IgG3

CHO cells were used to produce αCD47-G1, αCD47-G4, A4-IgG2b, and A4-IgG3 for functionality tests. The light chain and heavy chain coding genes of human αCD47-G4 were reconstructed into the lentivirus system, as reported previously.[47] To generate human αCD47-G1, the light chain coding gene of αCD47-G4 was employed, maintaining the variable region identical to that of human αCD47-G4. The IgG4 constant region was substituted with the IgG1 constant region. For A4-IgG2b and A4-IgG3, the DNA sequences encoding the anti-mouse CD47 VHH nanobody (clone A4) were fused with mouse IgG2b or IgG3, respectively. Lentiviral vectors were utilized to transduce CHO cells for expressing αCD47-G1, αCD47-G4, A4-IgG2b, or A4-IgG3.

In the case of αCD47-G1 and αCD47-G4, distinct lentiviral vectors carrying the light chain and heavy chain coding genes were used. GFP and mCherry served as selection markers, facilitating the sorting of double-positive CHO cells using a FACS Aria II cell sorter (BD Biosciences, San Jose, CA). For A4-IgG2b and A4-IgG3, the fusion protein was carried by the pCDH lentiviral vector with a GFP selection marker, transduced into CHO cells, and subsequently purified using a FACS Aria II cell sorter (BD Biosciences). The conditioned supernatants of lentivirus-infected CHO cells were employed to purify αCD47-G1, αCD47-G4, A4-IgG2b, and A4-IgG3 by utilizing a protein G column (Thermo Fisher Scientific, 89927).

CD47 binding and blocking assays

MDA-MB-231 cells, pre-treated with 2% BSA, were exposed to αCD47-G1 or αCD47-G4 antibodies purified from transduced CHO cells at concentrations ranging from 0 to 10,000 ng/mL for 30 min. Following this, the cells underwent two washes and were then stained with BV786-conjugated anti-human CD47 antibody (clone B6H12, BD Biosciences, 563758) for 20 min. Subsequently, flow cytometry analysis was performed using a Fortessa X20 flow cytometer (BD Biosciences).

Measurement of antibody concentration

MDA-MB-231 cells, either treated with or without TMZ, were exposed to OV-Q1, OV-αCD47-G1, or OV-αCD47-G4 at an MOI of 2. Two hours post-infection, the media were replaced with fresh media. Supernatants from each group were collected at 6, 12, 24, 48, and 72 hpi for antibody concentration measurement via ELISA. Standard amounts of αCD47-G1 and αCD47-G4 antibodies, purified from transduced CHO cells and with known concentrations, were used as references. ELISA was performed with slight modification.[48]

oHSV generation, expansion, and titration

OV-αCD47-G1 and OV-αCD47-G4, along with OV-A4-IgG2b and OV-A4-IgG3, were produced as reported previously.[6,12] In brief, the antibody sequences were inserted into pT-oriSIE4/5 following the HSV pIE4/5 promoter to construct the shuttle plasmids. The shuttle plasmids were recombined with fHsvQuik-1 for engineering the oHSVs. Vero cells were utilized for the propagation and titration of the viruses. Virus titration was conducted through plaque assays. In brief, monolayer Vero cells were seeded in a 96-well plate. After 12 h, these cells were infected with gradient-diluted viral solutions. Following a 2-h infection, the infection media were replaced with DMEM supplemented with 10% FBS. GFP-positive plaques were observed and counted using a Zeiss fluorescence microscope (AXIO observer 7) 2 days after infection to determine the viral titer.

For the concentration and purification of viral particles, the culture media containing viruses were harvested and centrifuged at 3,000 × *g* for 30 min. Subsequently, the supernatants were collected and subjected to ultra-centrifugation at 100,000 × *g* for 1 h. The resulting virus pellets were resuspended with saline as needed.

Oncolysis and viral production assay

The *in vitro* oncolysis assay was measured by the CellTiter-Glo 2.0 assay with slight modification. The viral replication assay was performed by plaque assay.[49] In brief, monolayers of MDA-MB-231 cells treated with or without TMZ were seeded on 96-well plates and infected with OV-Q1, OV-αCD47-G1, or OV-αCD47-G4 at an MOI of 2. Two hours after infection, the infection medium was replaced with fresh medium. The supernatants from each group were then harvested at 72 hpi, and viral titers were determined by plaque assays.

Isolation and culture of macrophages

For isolating and culturing mouse BMDMs, BALB/c mice were sacrificed at the time of bone marrow harvest. Bone marrow cells were extracted from the tibias and femurs by flushing with culture medium using a 25-G needle. The cells were then passed through a 70-μm nylon mesh (BD Biosciences) and washed three times with PBS. Extracted BM cells were implanted with 2.4×10^7/100 mm culture dish (BD Falcon) and cultured for 7 days in the presence of mouse M-CSF (PeproTech, 315-02) medium (replacing culture medium on days 3 and 5).

For isolating and culturing human primary macrophages, peripheral blood was collected from healthy donors. Human monocytes were isolated and enriched by using the RosetteSep Human Monocyte Enrichment Cocktail kit (STEMCELL, cat. no. 15068) from peripheral blood. The enriched human monocytes were cultured with RPMI 1640 medium containing 20 ng/mL human M-CSF (PeproTech, cat. no. 300-25-50UG) and 2% human serum for 7 days to induce macrophage differentiation (replacing culture medium on days 3 and 5).

Flow cytometry-based phagocytosis assay

For the phagocytosis assay of mouse BMDMs, MDA-MB-231 cells pre-treated with or without TMZ and stained with CFSE (Thermo Fisher Scientific, C34554) were used as target cells for 6 h. BMDMs and pre-treated target cells were co-cultured at a ratio of 1:2 for 2 h in the presence of vehicle control, αCD47-G1, or αCD47-G4 at a dose of 5 μg/mL in a humidified 5% CO_2 incubator at 37°C in ultra-low-attachment 96-well U-bottom plates (Corning) in serum-free RPMI 1640 (Life Technologies). Then the cells were harvested by centrifuging at 400 × *g* for 5 min at 4°C and stained with anti-mouse CD11b (BD Biosciences, 552850) to identify macrophages. To detect the effect of A4-IgG2b and A4-IgG3 on phagocytosis of BMDMs against mouse breast cancer cells we pre-treated the mouse breast cancer cell line E0771 with or without TMZ for 6 h. The pre-treated E0771 target cells were then incubated with PBS vehicle control, A4-IgG2b, or A4-IgG3 produced by CHO cells at a concentration of 5 μg/mL, following the similar procedures mentioned above. All flow cytometry data were collected using a Fortessa X20 flow cytometer (BD Biosciences). Phagocytosis was measured as the number of $CD11b^+CFSE^+$ macrophages, quantified as a percentage of the total $CD11b^+$ macrophages.

For the phagocytosis assay of human primary macrophages, MDA-MB-231 cells pre-treated with or without TMZ and stained with CFSE (Thermo Fisher Scientific, C34554) were used as target cells. Human macrophages and target cells were co-cultured at a ratio of 1:2 for 4 h in the presence of vehicle control, αCD47-G1, or αCD47-G4 produced by CHO cells at a dose of 5 μg/mL in a humidified 5% CO_2 incubator at 37°C in ultra-low-attachment 96-well U-bottom plates (Corning) in serum-free RPMI 1640 (Life Technologies). Then the cells were harvested by centrifuging at 400 × *g* for 5 min at 4°C and stained with anti-human CD11b (BD Biosciences, 552850, 5 μL/sample) to identify macrophages. All flow cytometry data were collected using a Fortessa X20 flow cytometer (BD Biosciences) with BD FACSDiva v.6 software (BD Biosciences). Phagocytosis was measured as the number of $CD11b^+CFSE^+$ macrophages, quantified as a percentage of the total $CD11b^+$ macrophages.

NK cell cytotoxicity and activation assay

MDA-MB-231 and E0771 cells were used as target cells. Primary human NK cells isolated from leukocyte cones of healthy donors using an NK cell isolation kit (MACSxpress Miltenyi Biotec, San Diego, CA) and an erythrocyte depletion kit (Miltenyi Biotec) were used as effector cells. The target cells were labeled with ^{51}Cr for 1 h. MDA-MB-231 cells treated with TMZ were co-cultured with 1 μg/mL αCD47-G1 or αCD47-G4 antibodies or vehicle for 30 min. Then the target cells were co-cultured with isolated human primary NK cells at different effector to target ratios at 37°C for 4 h. ^{51}Cr release was measured with a MicroBeta^2 microplate radiometric counters (PerkinElmer, Waltham, MA). Target cells incubated in complete medium or 1% SDS medium were used for spontaneous or maximal ^{51}Cr release control, respectively. The cell lysis percentages were calculated using the standard formula: 100 × (cpm experimental release – cpm spontaneous release)/(cpm maximal release – cpm spontaneous release). The assays were performed in at least three technical replicates with NK cells from different donors. Following a 4-h co-culture of NK cells and MDA-MB-231 cells at a ratio of 1:1, the expression of NK cell activation markers CD69 and CD107a was measured with a flow cytometer using the following antibodies: anti-CD56 (BD Biosciences, 557919, 5 μL/sample), anti-CD69 (BD Biosciences, 562883, 5 μL/sample), and CD107a (BD Biosciences, 555800, 10 μL/sample) antibodies. The granzyme B, TNF-α, and IFN-γ expression of NK cells was measured using the anti-granzyme B antibody (Invitrogen, 25-7349-82, 5 μL/sample), anti-TNF-α, and anti-IFN-γ (BD Biosciences, 554551, 5 μL/sample) antibodies.

qPCR

To assess the impact of αCD47-G1, αCD47-G4, OV-αCD47-G1, or OV-αCD47-G4 on activating the transcription of typical mouse macrophage cytokine genes, mouse BMDMs and MDA-MB-231 cells, treated with or without TMZ, were co-cultured at a ratio of 1:1 for 6 h. This was done with or without the presence of 5 μg/mL αCD47-G1, 5 μg/mL αCD47-G4, or the conditioned medium of OV-αCD47-G1 or OV-αCD47-G4. Subsequently, total RNA was extracted for reverse transcription to generate cDNA, enabling the detection of relative mRNA transcription levels of mouse Ccl2, Ccl4, Il1b, Il6, Il12b, and Nos2 genes using corresponding primers. The internal control used was 18s rRNA.

For evaluating the effect of αCD47-G1 or αCD47-G4 produced by CHO cells or supernatants of OV-αCD47-G1- or OV-αCD47-G4-infected MDA-MB-231 cells on activating transcription of typical human macrophage cytokine genes, human macrophages and MDA-MB-231 cells, pre-treated with or without TMZ as described above, were co-cultured at a ratio of 1:1 for 6 h. This was performed with or without the presence of 5 μg/mL αCD47-G1, 5 μg/mL αCD47-G4, or the conditioned medium of OV-αCD47-G1 or OV-αCD47-G4. The total RNA was then extracted for reverse transcription to generate cDNA for detecting relative mRNA transcription levels of human Il1b, Il6, and Nos2 genes using corresponding primers. 18s rRNA served as the internal control. Information about the primers used is provided in Table S1. The real-time PCR data were collected using the Applied Biosystems StepOnePlus real-time PCR system and QuantStudio 12K Flex software v.1.2.4.

Animal study

All animals in this study were accommodated at the City of Hope Animal Facility, adhering to a 12-h light/12-h dark cycle, and maintained

at temperatures ranging from 65°F to 75°F (~18°C–23°C) with humidity levels between 40% and 60%. Female athymic nude mice, aged 6–8 weeks, were procured from Jackson Laboratory (Bar Harbor, ME). In the survival studies, mice underwent anesthesia and were stereotactically injected with 1×10^5 MDA-MB-231 cells into the right frontal lobe of the brain (2 mm lateral and 1 mm anterior to bregma at a depth of 3 mm) on day 1. Subsequently, mice were randomly assigned to groups for i.c. injection on day 4, receiving either 2×10^5 PFU oHSV (OV-Q1, OV-αCD47-G1, or OV-αCD47-G4) in 3 μL of saline or saline alone as a control. From day 4 to 11, mice were intraperitoneally injected with TMZ. Disease progression was closely monitored through frequent weight measurements. Moribund mice, exhibiting neurological impairments and significant weight loss, were euthanized.

For establishing the immunocompetent mouse BCBM model, 6- to 8-week-old female and male C57BL/6 mice were purchased from Jackson Laboratory and housed at the City of Hope Animal Facility. Mice were anesthetized and stereotactically injected with 1×10^5 E0771 cells into the right frontal lobe of the brain (2 mm lateral and 1 mm anterior to bregma at a depth of 3 mm). The cells grew for 3 days, and animals were randomly divided into groups that were i.c. injected with 2×10^5 PFU oHSV (OV-Q1, OV-A4-IgG2b, or OV-A4-IgG3) in 3 μL of saline or saline alone as control. Mice were intraperitoneally injected with TMZ from day 3 to 10. Mice were subsequently monitored and weighed frequently for BCBM disease progression.

Flow cytometry

Mononuclear cells in the brain were extracted with Percoll and stained with anti-NKp46 (BioLegend, 137618, 5 μL/sample), anti-CD3 (BD Biosciences, 553066, 5 μL/sample), anti-CD45 (BD Biosciences, 559864, 5 μL/sample), anti-CD11b (BD Biosciences, 552850, 5 μL/sample), anti-F4/80 (Thermo Fisher Scientific, 12-4801-82, 5 μL/sample), anti-CD206 (BioLegend, 141734, 5 μL/sample), and anti-CD69 (BD Biosciences, 564683, 5 μL/sample) antibodies for flow cytometric analysis of immune cell brain infiltration and activation. The flow cytometric assessments of mouse immune cells were performed with at least four independent animals. All flow cytometry data were collected using the Fortessa X-20 flow cytometer.

Statistical analysis

Descriptive statistics (means, standard deviations, median, counts, etc.) are used to summarize data. Continuous endpoints that are normally distributed with or without prior log transformation were compared between two or more independent conditions by Student's t test or one-way ANOVA, respectively. For data with repeated measures from the same subject/donor, a linear mixed model was used to compare matched groups by accounting for the underlying variance and covariance structure. *p* values were adjusted for multiple comparisons by Holm's procedure or the Bonferroni method. For survival data, survival functions were estimated by the Kaplan-Meier method and compared by log rank test. All tests were two sided. A *p* value of 0.05 or less was defined as statistically significant. Statistical software GraphPad, R.3.6.3., and SAS 9.4 were used for the statistical analysis.

DATA AND CODE AVAILABILITY

All original data underlying selected data shown in the figures and supplemental figures are available from the corresponding authors upon reasonable request.

SUPPLEMENTAL INFORMATION

Supplemental information can be found online at https://doi.org/10.1016/j.omton.2024.200824.

ACKNOWLEDGMENTS

This work was supported by a 2021 Exceptional Project Award from the Breast Cancer Alliance (to J.Y.) and grants from the NIH (NS106170, AI129582, CA247550, CA264512, CA266457, CA223400, CA210087, CA265095, and CA163205).

AUTHOR CONTRIBUTIONS

J.Y. and M.A.C. conceived and designed the project. J.W., L.T., L.J., Y.C., Z.L., G.W., J.-C.L., and L.-S.L. conducted experiments. T.B., L.T., and J.Z. performed data analyses. J.W., T.B., L.T., and J.Y. wrote the paper. D.H., M.F., J.Y., and M.A.C. revised the paper. J.Y. and M.A.C. acquired funding. All authors discussed the results and commented on the manuscript.

DECLARATION OF INTERESTS

M.A.C. and J.Y. have relevant or non-relevant oncolytic virus patents pending.

REFERENCES

1. Duggan, C., Trapani, D., Ilbawi, A.M., Fidarova, E., Laversanne, M., Curigliano, G., Bray, F., and Anderson, B.O. (2021). National health system characteristics, breast cancer stage at diagnosis, and breast cancer mortality: a population-based analysis. Lancet Oncol. *22*, 1632–1642. https://doi.org/10.1016/S1470-2045(21)00462-9.

2. Freedman, R.A., Gelman, R.S., Anders, C.K., Melisko, M.E., Parsons, H.A., Cropp, A.M., Silvestri, K., Cotter, C.M., Componeschi, K.P., Marte, J.M., et al. (2019). TBCRC 022: A Phase II Trial of Neratinib and Capecitabine for Patients With Human Epidermal Growth Factor Receptor 2-Positive Breast Cancer and Brain Metastases. J. Clin. Oncol. *37*, 1081–1089. https://doi.org/10.1200/JCO.18.01511.

3. Lin, N.U., Pegram, M., Sahebjam, S., Ibrahim, N., Fung, A., Cheng, A., Nicholas, A., Kirschbrown, W., and Kumthekar, P. (2021). Pertuzumab Plus High-Dose Trastuzumab in Patients With Progressive Brain Metastases and HER2-Positive Metastatic Breast Cancer: Primary Analysis of a Phase II Study. J. Clin. Oncol. *39*, 2667–2675. https://doi.org/10.1200/JCO.20.02822.

4. Martin, A.M., Cagney, D.N., Catalano, P.J., Warren, L.E., Bellon, J.R., Punglia, R.S., Claus, E.B., Lee, E.Q., Wen, P.Y., Haas-Kogan, D.A., et al. (2017). Brain Metastases in Newly Diagnosed Breast Cancer: A Population-Based Study. JAMA Oncol. *3*, 1069–1077. https://doi.org/10.1001/jamaoncol.2017.0001.

5. Ippen, F.M., Grosch, J.K., Subramanian, M., Kuter, B.M., Liederer, B.M., Plise, E.G., Mora, J.L., Nayyar, N., Schmidt, S.P., Giobbie-Hurder, A., et al. (2019). Targeting the PI3K/Akt/mTOR pathway with the pan-Akt inhibitor GDC-0068 in PIK3CA-mutant breast cancer brain metastases. Neuro. Oncol. *21*, 1401–1411. https://doi.org/10.1093/neuonc/noz105.

6. Xu, B., Tian, L., Chen, J., Wang, J., Ma, R., Dong, W., Li, A., Zhang, J., Antonio Chiocca, E., Kaur, B., et al. (2021). An oncolytic virus expressing a full-length antibody enhances antitumor innate immune response to glioblastoma. Nat. Commun. *12*, 5908. https://doi.org/10.1038/s41467-021-26003-6.

7. McGrail, D.J., Pilié, P.G., Rashid, N.U., Voorwerk, L., Slagter, M., Kok, M., Jonasch, E., Khasraw, M., Heimberger, A.B., Lim, B., et al. (2021). High tumor mutation burden fails to predict immune checkpoint blockade response across all cancer types. Ann. Oncol. *32*, 661–672. https://doi.org/10.1016/j.annonc.2021.02.006.

8. Schlam, I., and Gatti-Mays, M.E. (2022). Immune Checkpoint Inhibitors in the Treatment of Breast Cancer Brain Metastases. Oncologist *27*, 538–547. https://doi.org/10.1093/oncolo/oyac064.

9. Nanda, R., Chow, L.Q.M., Dees, E.C., Berger, R., Gupta, S., Geva, R., Pusztai, L., Pathiraja, K., Aktan, G., Cheng, J.D., et al. (2016). Pembrolizumab in Patients With Advanced Triple-Negative Breast Cancer: Phase Ib KEYNOTE-012 Study. J. Clin. Oncol. *34*, 2460–2467. https://doi.org/10.1200/jco.2015.64.8931.

10. Cortes, J., Rugo, H.S., Cescon, D.W., Im, S.A., Yusof, M.M., Gallardo, C., Lipatov, O., Barrios, C.H., Perez-Garcia, J., Iwata, H., et al. (2022). Pembrolizumab plus Chemotherapy in Advanced Triple-Negative Breast Cancer. N. Engl. J. Med. *387*, 217–226. https://doi.org/10.1056/NEJMoa2202809.

11. Wagner, J., Rapsomaniki, M.A., Chevrier, S., Anzeneder, T., Langwieder, C., Dykgers, A., Rees, M., Ramaswamy, A., Muenst, S., Soysal, S.D., et al. (2019). A Single-Cell Atlas of the Tumor and Immune Ecosystem of Human Breast Cancer. Cell *177*, 1330–1345.e18. https://doi.org/10.1016/j.cell.2019.03.005.

12. Tian, L., Xu, B., Teng, K.Y., Song, M., Zhu, Z., Chen, Y., Wang, J., Zhang, J., Feng, M., Kaur, B., et al. (2022). Targeting Fc Receptor-Mediated Effects and the "Don't Eat Me" Signal with an Oncolytic Virus Expressing an Anti-CD47 Antibody to Treat Metastatic Ovarian Cancer. Clin. Cancer Res. *28*, 201–214. https://doi.org/10.1158/1078-0432.CCR-21-1248.

13. Liu, D., Lu, Q., Wang, X., Wang, J., Lu, N., Jiang, Z., Hao, X., Li, J., Liu, J., Cao, P., et al. (2019). LSECtin on tumor-associated macrophages enhances breast cancer stemness via interaction with its receptor BTN3A3. Cell Res. *29*, 365–378. https://doi.org/10.1038/s41422-019-0155-6.

14. Mahmoud, S.M.A., Lee, A.H.S., Paish, E.C., Macmillan, R.D., Ellis, I.O., and Green, A.R. (2012). Tumour-infiltrating macrophages and clinical outcome in breast cancer. J. Clin. Pathol. *65*, 159–163. https://doi.org/10.1136/jclinpath-2011-200355.

15. Leek, R.D., Hunt, N.C., Landers, R.J., Lewis, C.E., Royds, J.A., and Harris, A.L. (2000). Macrophage infiltration is associated with VEGF and EGFR expression in breast cancer. J. Pathol. *190*, 430–436. https://doi.org/10.1002/(SICI)1096-9896(200003)190:4<430::AID-PATH538>3.0.CO;2-6.

16. Cao, X., Li, B., Chen, J., Dang, J., Chen, S., Gunes, E.G., Xu, B., Tian, L., Muend, S., Raoof, M., et al. (2021). Effect of cabazitaxel on macrophages improves CD47-targeted immunotherapy for triple-negative breast cancer. J. Immunother. Cancer *9*, e002022. https://doi.org/10.1136/jitc-2020-002022.

17. Jiang, Z., Sun, H., Yu, J., Tian, W., and Song, Y. (2021). Targeting CD47 for cancer immunotherapy. J. Hematol. Oncol. *14*, 180. https://doi.org/10.1186/s13045-021-01197-w.

18. Upton, R., Banuelos, A., Feng, D., Biswas, T., Kao, K., McKenna, K., Willingham, S., Ho, P.Y., Rosental, B., Tal, M.C., et al. (2021). Combining CD47 blockade with trastuzumab eliminates HER2-positive breast cancer cells and overcomes trastuzumab tolerance. Proc. Natl. Acad. Sci. USA *118*, e2026849118. https://doi.org/10.1073/pnas.2026849118.

19. Ma, R., Li, Z., Chiocca, E.A., Caligiuri, M.A., and Yu, J. (2023). The emerging field of oncolytic virus-based cancer immunotherapy. Trends Cancer *9*, 122–139. https://doi.org/10.1016/j.trecan.2022.10.003.

20. Tian, L., Xu, B., Chen, Y., Li, Z., Wang, J., Zhang, J., Ma, R., Cao, S., Hu, W., Chiocca, E.A., et al. (2022). Specific targeting of glioblastoma with an oncolytic virus expressing a cetuximab-CCL5 fusion protein via innate and adaptive immunity. Nat. Cancer *3*, 1318–1335. https://doi.org/10.1038/s43018-022-00448-0.

21. Saha, D., Rabkin, S.D., and Martuza, R.L. (2020). Temozolomide antagonizes oncolytic immunovirotherapy in glioblastoma. J. Immunother. Cancer *8*, e000345. https://doi.org/10.1136/jitc-2019-000345.

22. Thomas, S., Kuncheria, L., Roulstone, V., Kyula, J.N., Mansfield, D., Bommareddy, P.K., Smith, H., Kaufman, H.L., Harrington, K.J., and Coffin, R.S. (2019). Development of a new fusion-enhanced oncolytic immunotherapy platform based on herpes simplex virus type 1. J. Immunother. Cancer *7*, 214. https://doi.org/10.1186/s40425-019-0682-1.

23. Hegi, M.E., Diserens, A.C., Gorlia, T., Hamou, M.F., de Tribolet, N., Weller, M., Kros, J.M., Hainfellner, J.A., Mason, W., Mariani, L., et al. (2005). MGMT gene silencing and benefit from temozolomide in glioblastoma. N. Engl. J. Med. *352*, 997–1003. https://doi.org/10.1056/NEJMoa043331.

24. Karachi, A., Dastmalchi, F., Mitchell, D.A., and Rahman, M. (2018). Temozolomide for immunomodulation in the treatment of glioblastoma. Neuro. Oncol. *20*, 1566–1572. https://doi.org/10.1093/neuonc/noy072.

25. Kanai, R., Rabkin, S.D., Yip, S., Sgubin, D., Zaupa, C.M., Hirose, Y., Louis, D.N., Wakimoto, H., and Martuza, R.L. (2012). Oncolytic virus-mediated manipulation of DNA damage responses: synergy with chemotherapy in killing glioblastoma stem cells. J. Natl. Cancer Inst. *104*, 42–55. https://doi.org/10.1093/jnci/djr509.

26. Fan, J., Jiang, H., Cheng, L., Ma, B., and Liu, R. (2021). Oncolytic herpes simplex virus and temozolomide synergistically inhibit breast cancer cell tumorigenesis in vitro and in vivo. Oncol. Lett. *21*, 99. https://doi.org/10.3892/ol.2020.12360.

27. Lee, S.Y. (2016). Temozolomide resistance in glioblastoma multiforme. Genes Dis. *3*, 198–210. https://doi.org/10.1016/j.gendis.2016.04.007.

28. Kinder, M., Greenplate, A.R., Strohl, W.R., Jordan, R.E., and Brezski, R.J. (2015). An Fc engineering approach that modulates antibody-dependent cytokine release without altering cell-killing functions. MAbs *7*, 494–504. https://doi.org/10.1080/19420862.2015.1022692.

29. Weischenfeldt, J., and Porse, B. (2008). Bone Marrow-Derived Macrophages (BMM): Isolation and Applications. CSH Protoc. *2008*, pdb.prot5080. https://doi.org/10.1101/pdb.prot5080.

30. Gupta, S.K., Kizilbash, S.H., Carlson, B.L., Mladek, A.C., Boakye-Agyeman, F., Bakken, K.K., Pokorny, J.L., Schroeder, M.A., Decker, P.A., Cen, L., et al. (2016). Delineation of MGMT Hypermethylation as a Biomarker for Veliparib-Mediated Temozolomide-Sensitizing Therapy of Glioblastoma. J. Natl. Cancer Inst. *108*, djv369. https://doi.org/10.1093/jnci/djv369.

31. Sockolosky, J.T., Dougan, M., Ingram, J.R., Ho, C.C.M., Kauke, M.J., Almo, S.C., Ploegh, H.L., and Garcia, K.C. (2016). Durable antitumor responses to CD47 blockade require adaptive immune stimulation. Proc. Natl. Acad. Sci. USA *113*, E2646–E2654. https://doi.org/10.1073/pnas.1604268113.

32. Gholamin, S., Youssef, O.A., Rafat, M., Esparza, R., Kahn, S., Shahin, M., Giaccia, A.J., Graves, E.E., Weissman, I., Mitra, S., and Cheshier, S.H. (2020). Irradiation or temozolomide chemotherapy enhances anti-CD47 treatment of glioblastoma. Innate Immun. *26*, 130–137. https://doi.org/10.1177/1753425919876690.

33. Cao, K.I., Lebas, N., Gerber, S., Levy, C., Le Scodan, R., Bourgier, C., Pierga, J.Y., Gobillion, A., Savignoni, A., and Kirova, Y.M. (2015). Phase II randomized study of whole-brain radiation therapy with or without concurrent temozolomide for brain metastases from breast cancer. Ann. Oncol. *26*, 89–94. https://doi.org/10.1093/annonc/mdu488.

34. van den Bent, M.J., Tesileanu, C.M.S., Wick, W., Sanson, M., Brandes, A.A., Clement, P.M., Erridge, S., Vogelbaum, M.A., Nowak, A.K., Baurain, J.F., et al. (2021). Adjuvant and concurrent temozolomide for 1p/19q non-co-deleted anaplastic glioma (CATNON; EORTC study 26053-22054): second interim analysis of a randomised, open-label, phase 3 study. Lancet Oncol. *22*, 813–823. https://doi.org/10.1016/S1470-2045(21)00090-5.

35. Weller, J., Tzaridis, T., Mack, F., Steinbach, J.P., Schlegel, U., Hau, P., Krex, D., Grauer, O., Goldbrunner, R., Bähr, O., et al. (2019). Health-related quality of life and neurocognitive functioning with lomustine-temozolomide versus temozolomide in patients with newly diagnosed, MGMT-methylated glioblastoma (CeTeG/NOA-09): a randomised, multicentre, open-label, phase 3 trial. Lancet Oncol. *20*, 1444–1453. https://doi.org/10.1016/S1470-2045(19)30502-9.

36. Chao, M.P., Jaiswal, S., Weissman-Tsukamoto, R., Alizadeh, A.A., Gentles, A.J., Volkmer, J., Weiskopf, K., Willingham, S.B., Raveh, T., Park, C.Y., et al. (2010). Calreticulin is the dominant pro-phagocytic signal on multiple human cancers and is counterbalanced by CD47. Sci. Transl. Med. *2*, 63ra94. https://doi.org/10.1126/scitranslmed.3001375.

37. Wang, J., and Matosevic, S. (2020). Functional and metabolic targeting of natural killer cells to solid tumors. Cell. Oncol. *43*, 577–600. https://doi.org/10.1007/s13402-020-00523-7.

38. Zhang, J., Stevens, M.F.G., and Bradshaw, T.D. (2012). Temozolomide: mechanisms of action, repair and resistance. Curr. Mol. Pharmacol. *5*, 102–114. https://doi.org/10.2174/1874467211205010102.

39. Ellul, M., and Solomon, T. (2018). Acute encephalitis - diagnosis and management. Clin. Med. *18*, 155–159. https://doi.org/10.7861/clinmedicine.18-2-155.

40. Deuse, T., Hu, X., Agbor-Enoh, S., Jang, M.K., Alawi, M., Saygi, C., Gravina, A., Tediashvili, G., Nguyen, V.Q., Liu, Y., et al. (2021). The SIRPα-CD47 immune checkpoint in NK cells. J. Exp. Med. *218*, e20200839. https://doi.org/10.1084/jem.20200839.

41. Guadagno, E., Presta, I., Maisano, D., Donato, A., Pirrone, C.K., Cardillo, G., Corrado, S.D., Mignogna, C., Mancuso, T., Donato, G., et al. (2018). Role of Macrophages in Brain Tumor Growth and Progression. Int. J. Mol. Sci. *19*, 1005. https://doi.org/10.3390/ijms19041005.

42. von Roemeling, C.A., Wang, Y., Qie, Y., Yuan, H., Zhao, H., Liu, X., Yang, Z., Yang, M., Deng, W., Bruno, K.A., et al. (2020). Therapeutic modulation of phagocytosis in glioblastoma can activate both innate and adaptive antitumour immunity. Nat. Commun. *11*, 1508. https://doi.org/10.1038/s41467-020-15129-8.

43. Luo, B., and Lee, A.S. (2013). The critical roles of endoplasmic reticulum chaperones and unfolded protein response in tumorigenesis and anticancer therapies. Oncogene *32*, 805–818. https://doi.org/10.1038/onc.2012.130.

44. Salazar, N., Carlson, J.C., Huang, K., Zheng, Y., Oderup, C., Gross, J., Jang, A.D., Burke, T.M., Lewén, S., Scholz, A., et al. (2018). A Chimeric Antibody against ACKR3/CXCR7 in Combination with TMZ Activates Immune Responses and Extends Survival in Mouse GBM Models. Mol. Ther. *26*, 1354–1365. https://doi.org/10.1016/j.ymthe.2018.02.030.

45. Wang, J., Toregrosa-Allen, S., Elzey, B.D., Utturkar, S., Lanman, N.A., Bernal-Crespo, V., Behymer, M.M., Knipp, G.T., Yun, Y., Veronesi, M.C., et al. (2021). Multispecific targeting of glioblastoma with tumor microenvironment-responsive multifunctional engineered NK cells. Proc. Natl. Acad. Sci. USA *118*, e2107507118. https://doi.org/10.1073/pnas.2107507118.

46. Chang, D.Y., Jung, J.H., Kim, A.A., Marasini, S., Lee, Y.J., Paek, S.H., Kim, S.S., and Suh-Kim, H. (2020). Combined effects of mesenchymal stem cells carrying cytosine deaminase gene with 5-fluorocytosine and temozolomide in orthotopic glioma model. Am. J. Cancer Res. *10*, 1429–1441.

47. Liu, J., Wang, L., Zhao, F., Tseng, S., Narayanan, C., Shura, L., Willingham, S., Howard, M., Prohaska, S., Volkmer, J., et al. (2015). Pre-Clinical Development of a Humanized Anti-CD47 Antibody with Anti-Cancer Therapeutic Potential. PLoS One *10*, e0137345. https://doi.org/10.1371/journal.pone.0137345.

48. Chen, L., Mao, H., Zhang, J., Chu, J., Devine, S., Caligiuri, M.A., and Yu, J. (2017). Targeting FLT3 by chimeric antigen receptor T cells for the treatment of acute myeloid leukemia. Leukemia *31*, 1830–1834. https://doi.org/10.1038/leu.2017.147.

49. Xu, B., Ma, R., Russell, L., Yoo, J.Y., Han, J., Cui, H., Yi, P., Zhang, J., Nakashima, H., Dai, H., et al. (2018). An oncolytic herpesvirus expressing E-cadherin improves survival in mouse models of glioblastoma. Nat. Biotechnol. *31*, 1830. https://doi.org/10.1038/nbt.4302.